

A finite size scaling study of lattice models in the three-dimensional Ising universality class

Martin Hasenbusch*

*Institut für Physik, Humboldt-Universität zu Berlin,
Newtonstr. 15, 12489 Berlin, Germany*

(Dated: March 25, 2011)

Abstract

We study the spin-1/2 Ising model and the Blume-Capel model at various values of the parameter D on the simple cubic lattice. To this end we perform Monte Carlo simulations using a hybrid of the local Metropolis, the single cluster and the wall cluster algorithm. Using finite size scaling we determine the value $D^* = 0.656(20)$ of the parameter D , where leading corrections to scaling vanish. We find $\omega = 0.832(6)$ for the exponent of leading corrections to scaling. In order to compute accurate estimates of critical exponents we construct improved observables that have a small amplitude of the leading correction for any model. Analyzing data obtained for $D = 0.641$ and 0.655 on lattices of a linear size up to $L = 360$ we obtain $\nu = 0.63002(10)$ and $\eta = 0.03627(10)$. We compare our results with those obtained from previous Monte Carlo simulations and high temperature series expansions of lattice models, by using field theoretic methods and experiments.

PACS numbers: 05.50.+q, 05.70.Jk, 64.60.F-

* Martin.Hasenbusch@physik.hu-berlin.de

I. INTRODUCTION

In the neighborhood of a second order phase transition various quantities diverge. For example the correlation length, which characterizes the decay of the two-point correlation function, behaves as

$$\xi = f_{\pm}|t|^{-\nu} \times \left(1 + b_{\pm}|t|^{\theta} + ct + d_{\pm}|t|^{\theta'} + e_{\pm}|t|^{2\theta} + \dots\right), \quad (1)$$

where $t = (T - T_c)/T_c$ is the reduced temperature, f_+ and f_- are the amplitudes in the high and the low temperature phase, respectively, and ν is the critical exponent of the correlation length. These power laws are affected by confluent corrections, such as $b_{\pm}|t|^{\theta}$, $d_{\pm}|t|^{\theta'}$, $e_{\pm}|t|^{2\theta}$, and non-confluent ones such as ct . Critical exponents such as ν and ratios of amplitudes such as f_+/f_- are universal. This means that they assume exactly the same value for any system within a given universality class. Also correction exponents such as $\theta = \omega\nu \approx 0.5$ and ratios of correction amplitudes as b_+/b_- are universal. A universality class is characterized by the dimension of the system, the range of the interaction and the symmetry of the order parameter. The critical exponents α of the specific heat, γ of the magnetic susceptibility, η of the two-point correlation function at the critical point, ν of the correlation length, δ of the magnetization at the critical temperature as a function of the external field and β of the spontaneous magnetization at a vanishing external field are related by so called scaling and hyperscaling relations. This allows to deduce all of them from two independent exponents. For reviews on critical phenomena and the Renormalization Group (RG) see e.g. [1–4].

Here we are concerned with three dimensions, short range interactions and a \mathbb{Z}_2 symmetry of the order parameter. The best known model undergoing a phase transition in this universality class is the spin-1/2 Ising model in three dimensions with nearest neighbor interactions. Therefore this universality class is called the three-dimensional Ising universality class. This universality class is supposed to be realized in a huge range of experimental systems: binary mixtures, uniaxial magnets or micellar systems; see e.g. [4–6]. Typically the estimates of critical exponents extracted from experimental data are less accurate than those obtained by using the theoretical methods discussed below. For example, recent experimental estimates obtained from turbidity data for a methanol-cyclohexane mixture are $\nu = 0.632(2)$ and $\eta = 0.041(5)$ [7].

Critical exponents and amplitude ratios have been computed by various theoretical methods such as field theoretic methods or high temperature series expansions and Monte Carlo simulations of lattice models. First let us briefly discuss results obtained by the ϵ -expansion [8], where the dimension d of the system is given by $d = 4 - \epsilon$ and the perturbative expansion in $d = 3$ [9]. The ϵ -expansion of critical exponents has been computed up to $O(\epsilon^5)$ [10] while the perturbative expansion in $d = 3$ has been computed up to seven loops [11] for the Ising universality class. Since both expansions are divergent, some kind of resummation is needed to extract numerical results for critical exponents. In the case of the ϵ -expansion the estimates reported in the literature are consistent among each other. As a representative result we report in table I the one of ref. [12]. In table I we also give results obtained from the perturbative expansion in $d = 3$ using different resummation techniques. For a more complete compilation see e.g. ref. [4]. In table I we give the exponents ν , η and the correction exponent ω , since these are directly computed by using field theoretic methods. In addition we report the value of γ that can be compared with the results of the high temperature series expansions reported below. Typically, the

TABLE I. Numerical results for the critical exponents ν , γ , η and ω obtained by using field theoretic methods. The list is by far not exhaustive. We try to give extreme examples; both concerning the values found as well as the quoted error bar. In the case of the ϵ -expansion we have taken the results that fulfil the boundary condition that for $\epsilon = 2$ the correct 2D Ising results are obtained.

| ref | year | Method | ν | γ | η | ω |
|------|------|-----------------|------------|------------|------------|-----------|
| [12] | 1998 | ϵ -exp | 0.6305(25) | 1.2380(50) | 0.0365(50) | 0.814(18) |
| [13] | 1991 | 3D exp | 0.630 | 1.238 | 0.0355 | 0.845 |
| [11] | 1991 | 3D exp | 0.6301(5) | 1.2378(6) | 0.0355(9) | |
| [12] | 1998 | 3D exp | 0.6304(13) | 1.2396(13) | 0.0335(25) | 0.799(11) |
| [14] | 1999 | 3D exp | 0.6305 | 1.241 | 0.0347(1) | 0.805 |
| [15] | 2001 | 3D exp | 0.6303(8) | 1.2403(8) | 0.0335(6) | 0.792(3) |
| [16] | 2008 | 3D exp | 0.6306(5) | 1.2411(6) | 0.0318(3) | 0.782(5) |

errors reported for the critical exponents obtained from the perturbative expansion in $d = 3$ are smaller than those obtained from the ϵ -expansion. While the estimates for ν are all consistent within the quoted errors, clear variations can be observed for η , γ and ω . For a discussion of the different resummation schemes that have been used, we refer the reader to ref. [16].

In table II we summarize recent results obtained from lattice models. For an exhaustive summary of previous works see ref. [4]. The authors of [17] have analyzed the high temperature series expansion of improved models on the simple cubic lattice up to $O(\beta^{25})$, where $\beta = 1/k_B T$ is the inverse temperature. One of these models is studied here using Monte Carlo simulations. Improved means that the amplitudes of leading corrections to scaling such as b_{\pm} in eq. (1) vanish. The authors of [18] have studied the high temperature series expansion of spin- S Ising models on the simple cubic and the body centered cubic lattice up to $O(\beta^{25})$. Note that in the spin- S Ising model the spin-variable might assume the values $-S, -S + 1, \dots, S - 1, S$. In ref. [19] the same authors have studied the ϕ^4 model on the simple cubic and the body centered cubic lattice also up to $O(\beta^{25})$. These results from high temperature series expansions are all compatible among each other. Note that these expansions were performed for lattice models with quite different Hamiltonians. Furthermore, there are results for both simple cubic and body centered cubic lattices. It is highly plausible that corrections to scaling have different amplitudes in these different models. Therefore the agreement of the results gives us confidence that there are no undetected systematic errors due to leading, or in the case of improved models, subleading corrections to scaling. The results for the exponents ν , γ and η obtained from the high temperature series expansion are clearly more precise than those obtained by using field theoretic methods. The results obtained for ν using field theoretic methods and high temperature series expansions of lattice models are consistent. In the case of γ and η some of the results obtained by resumming the perturbative expansion in three dimensions can be clearly ruled out by the high temperature series expansion. Unfortunately, the analysis of the high temperature series expansions does not provide an accurate estimate for the correction exponent ω .

Lattice models can also be studied by using Monte Carlo simulations. The finite size

TABLE II. Numerical results for the critical exponents ν , γ , η and ω obtained by analyzing high temperature series (HT) and Monte Carlo (MC) simulations of lattice models in the Ising universality class. In the case of the Monte Carlo (MC) simulations, some of the authors have quoted the statistical and the systematical errors of ν and η separately. The numbers marked by * are not directly given by the authors but are computed by using the scaling relation $\gamma = \nu(2 - \eta)$. Note that the error of γ is computed naively, assuming that the errors of ν and η are purely statistical and that the estimates of ν and η are uncorrelated. For an exhaustive summary of previous work see ref. [4].

| ref | year | Method | ν | γ | η | ω |
|------|------|--------|--------------|-------------|--------------|-----------|
| [17] | 2002 | HT | 0.63012(16) | 1.2373(2) | 0.03639(15) | 0.825(50) |
| [18] | 2002 | HT | 0.6299(2) | 1.2371(1) | 0.0360(8)* | – |
| [19] | 2005 | HT | 0.6301(2) | 1.2373(2) | 0.0363(9)* | – |
| [23] | 1999 | MC | 0.6294(5)[5] | 1.2353(21)* | 0.0374(6)[6] | 0.87(9) |
| [24] | 1999 | MC | 0.6298(2)[3] | 1.2365(11)* | 0.0366(6)[2] | – |
| [25] | 1999 | MC | 0.6296(3)[4] | 1.2367(15)* | 0.0358(4)[5] | 0.845(10) |
| [26] | 1999 | MC | 0.63032(56) | 1.2372(13)* | 0.0372(10) | 0.82(3) |
| [27] | 2003 | MC | 0.63020(12) | 1.2372(4)* | 0.0368(2) | 0.821(5) |

scaling (FSS) approach [20–22] is well suited to locate the critical temperature and to compute critical exponents. Typically one simulates the model directly at the critical point. The critical exponents are then extracted from the scaling of the observables with the lattice size. For example, at the critical temperature the magnetic susceptibility behaves as

$$\chi = aL^{2-\eta} \times (1 + bL^{-\omega} + cL^{-\omega'} + dL^{-2\omega} + \dots) + B \quad , \quad (2)$$

where B is an analytic background and L the linear size of a cubic lattice with periodic boundary conditions. An exhaustive summary of previous works is given in table 5 of ref. [4]. In table II we only quote recent works. In 1999 four finite size scaling studies of lattices models in the Ising universality class had been published. The results of these works are consistent among each other and the accuracy that had been achieved is similar to that of the field theoretic calculations. I like to mention that in [26] a special purpose computer for the cluster simulation of the Ising model had been used. In the most recent work [27], which provides the most accurate estimates so far, 11 different models were studied on lattices up to a linear site of $L = 128$. The results obtained for ν , γ and η are essentially consistent with those obtained from the high temperature series expansions. The estimate obtained for ω is more accurate than that of the high temperature series expansion and it is clearly larger than most of the estimates obtained from the perturbative expansion in three dimensions.

The purpose of the present work is to corroborate the lattice results discussed above. To this end we shall simulate lattices that are considerably larger than those of ref. [27]. Furthermore we shall use improved observables that have been applied in ref. [28] to study Ising models with quenched dilution. Here, improved means that the amplitude of the leading correction vanishes for any model. Since these observables are constructed numerically, in practice some residual amplitude remains. Using these improved observ-

ables in the study of improved models, leading corrections are highly suppressed, allowing us to ignore them in the finite size scaling analysis.

Accurate numerical estimates of critical exponents might serve as benchmark for future experiments, see e.g. [6], the analysis of the perturbative expansion in three dimensions, as discussed above, or new theoretical approaches such as new ideas in the so called exact renormalization group [29] or the Kallen-Lehmann approach [30].

The outline of the paper is the following. First we define the model and the observables that are studied. Then we discuss the Monte Carlo algorithm that has been used. We give the details of our numerical study. We estimate the fixed point values of the phenomenological couplings and the inverse transition temperatures. We give a numerical estimate of the correction exponent ω and obtain a new estimate of D^* , the value of the parameter where leading corrections to scaling vanish. Next we construct various improved observables. Based on this we compute estimates for the critical exponents ν and η .

II. THE MODEL

The spin-1/2 Ising model is characterized by the reduced Hamiltonian

$$H = -\beta \sum_{\langle xy \rangle} s_x s_y - h \sum_x s_x \quad , \quad (3)$$

where the spin might assume the values $s_x \in \{-1, 1\}$. $x = (x_0, x_1, x_2)$ denotes a site of the simple cubic lattice, where $x_i \in \{0, 1, 2, \dots, L_i - 1\}$. $\langle xy \rangle$ denotes a pair of nearest neighbors on the lattice. We employ periodic boundary conditions in all directions of the lattice. Throughout we shall consider $L_0 = L_1 = L_2 = L$ and a vanishing external field $h = 0$. The partition function is given by

$$Z = \sum_{\{s_x\}} \exp(-H) \quad , \quad (4)$$

where $\sum_{\{s_x\}}$ denotes the sum over all configurations.

The Blume-Capel model is characterized by the reduced Hamiltonian

$$H = -\beta \sum_{\langle xy \rangle} s_x s_y + D \sum_x s_x^2 - h \sum_x s_x \quad , \quad (5)$$

where now the spin might assume the values $s_x \in \{-1, 0, 1\}$. In the limit $D \rightarrow -\infty$ the “state” $s = 0$ is completely suppressed, compared with $s = \pm 1$, and therefore the spin-1/2 Ising model is recovered. In $d \geq 2$ dimensions the model undergoes a continuous phase transition for $-\infty \leq D < D_{tri}$ at a β_c that depends on D . For $D > D_{tri}$ the model undergoes a first order phase transition. Refs. [31–33] give for the three-dimensional simple cubic lattice $D_{tri} \approx 2.006$, $D_{tri} \approx 2.05$ and $D_{tri} = 2.0313(4)$, respectively.

Numerically it has been shown that on the line of second order phase transitions there is a point, where leading corrections to scaling vanish. In the following we shall call the model at this point “improved model”. In ref. [34] we find $D^* = 0.641(8)$. One should note that no effort was made to estimate the systematical error due to subleading corrections to scaling. The authors of [27, 35] have simulated the model at $D = \ln 2 = 0.693147\dots$.

At this value of D corrections to scaling are still small compared with the spin-1/2 Ising model. At $D = \ln 2$ the Blume-Capel model can be mapped into a spin-1/2 Ising model with twice the number of sites. This model can be simulated with a cluster algorithm without additional local updates as it is the case for general values of D .

III. THE OBSERVABLES

The energy of a given spin configuration is defined as

$$E = \sum_{\langle xy \rangle} s_x s_y . \quad (6)$$

This definition is convenient for our purpose. One should note however that it deviates from the standard textbook definition. The magnetic susceptibility χ and the second moment correlation length ξ_{2nd} are defined as

$$\chi \equiv \frac{1}{V} \left\langle \left(\sum_x s_x \right)^2 \right\rangle , \quad (7)$$

where $V = L^3$ and

$$\xi_{2nd} \equiv \sqrt{\frac{\chi/F - 1}{4 \sin^2 \pi/L}} , \quad (8)$$

where

$$F \equiv \frac{1}{V} \left\langle \left| \sum_x \exp \left(i \frac{2\pi x_k}{L} \right) s_x \right|^2 \right\rangle \quad (9)$$

is the Fourier transform of the correlation function at the lowest non-zero momentum. In our simulations, we have measured F for the three directions $k = 0, 1, 2$ and have averaged these three results.

In addition to elementary quantities like the energy, the magnetization, the specific heat or the magnetic susceptibility, we compute a number of so-called phenomenological couplings, that means quantities that, in the critical limit, are invariant under RG transformations. We consider the Binder parameter U_4 and its sixth-order generalization U_6 , defined as

$$U_{2j} \equiv \frac{\langle m^{2j} \rangle}{\langle m^2 \rangle^j}, \quad (10)$$

where $m = \frac{1}{V} \sum_x s_x$ is the magnetization of a given spin configuration. We also consider the ratio $R_Z \equiv Z_a/Z_p$ of the partition function Z_a of a system with anti-periodic boundary conditions in one of the three directions and the partition function Z_p of a system with periodic boundary conditions in all directions. Anti-periodic boundary conditions in the zero direction are obtained by replacing $s_x s_y$ by $-s_x s_y$ in the Hamiltonian for links $\langle xy \rangle$ that connect the boundaries, i.e., for $x = (L-1, x_1, x_2)$ and $y = (0, x_1, x_2)$. The ratio Z_a/Z_p can be efficiently evaluated using the boundary flip algorithm [36]. Here we use a modified version of the boundary flip algorithm as discussed in appendix A 2 of ref. [37]. In the following we shall refer to the RG-invariant quantities U_{2j} , $R_Z \equiv Z_a/Z_p$ and $R_\xi \equiv \xi_{2nd}/L$ using the symbol R .

In our analysis we need the observables as a function of β in some neighborhood of the simulation point. To this end we have computed the coefficients of the Taylor expansion of the observables up to the third order. For example the first derivative of the expectation value $\langle A \rangle$ of an observable A is given by

$$\frac{\partial \langle A \rangle}{\partial \beta} = \langle AE \rangle - \langle A \rangle \langle E \rangle . \quad (11)$$

IV. THE SIMULATION ALGORITHM

Analogous to [38], we have simulated the Blume-Capel model using a hybrid of local updates and cluster updates. The cluster algorithm only changes the sign of spins. Therefore, in order to get an ergodic algorithm for the Blume-Capel model with finite D , local Metropolis updates are used that also can change the modulus $|s_x|$ of the spins. Following [39] even in the case of the spin-1/2 Ising model such a hybrid of local and cluster updates is superior to the cluster algorithm alone. The authors of [39] also found that such a hybrid algorithm is much less susceptible to systematic errors caused by the imperfection of pseudo-random numbers than a pure cluster algorithm. Here we have used a hybrid of local Metropolis updates that are implemented by using the multispin coding technique [40], single cluster updates [41] and wall cluster updates [42]. In the single cluster update, the cluster that includes a randomly chosen site is flipped. In contrast, in the wall cluster update all clusters that include sites that are part of a given plane (the "wall") of the lattice are flipped.

Motivated by the multispin coding implementation of the local update we have simulated $N_{bit} = 64$ copies of the system in parallel. In the first stage of our study, we have used a single random number sequence for the local Metropolis updates of these N_{bit} systems. This leads to some degradation of the performance. To diminish this problem, we have used a modified sequence of the pseudo random numbers in the second stage of our study. Details are given below. In the case of the cluster updates we could not make use of the multispin coding technique. Therefore we have updated the systems one by one, using different random number sequences for each of the systems.

Let us discuss the implementation of the local Metropolis algorithm in more detail. We have implemented the spin $s_x \in \{-1, 0, 1\}$ using two bits. To this end we write $s_x = \sigma_x \tau_x$, where $\sigma_x \in \{-1, 1\}$ and $\tau_x \in \{0, 1\}$. In terms of these new variables the partition function becomes

$$Z = C \sum_{\{\sigma_x\}} \sum_{\{\tau_x\}} \exp \left(\beta \sum_{\langle xy \rangle} \sigma_x \sigma_y \tau_x \tau_y - \tilde{D} \sum_x \tau_x \right) , \quad (12)$$

where $\tilde{D} = D - \ln 2$. Note that subtracting $\ln 2$ corrects for the double counting of the $s_x = 0$ state.

In our local updating scheme we performed consecutive updates of σ_x and τ_x . In the first step, the proposal is given by $\sigma'_x = -\sigma_x$. It is accepted with the standard Metropolis acceptance probability

$$P_{acc} = \min \left[1, \exp \left(-2\beta \sigma_x \tau_x \sum_{y.nn.x} \sigma_y \tau_y \right) \right] , \quad (13)$$

where $y.nn.x$ means that y is a nearest neighbor of x . In the second step, the proposal is given by $\tau'_x = 1 - \tau_x$. A natural choice for the acceptance is

$$P_{acc} = \min \left[1, \exp \left((2\tau_x - 1) \left[-\beta\sigma_x \sum_{y.nn.x} \sigma_y \tau_y + \tilde{D} \right] \right) \right] . \quad (14)$$

Instead, for technical reasons we have implemented a two stage acceptance step. For $D = 0.641$ and $D = 0.655$, where $|\tilde{D}|$ is small, we have chosen

$$P_{acc,1} = \min \left[1, \exp \left(\beta(1 - 2\tau_x)\sigma_x \sum_{y.nn.x} \sigma_y \tau_y \right) \right] \quad (15)$$

and

$$P_{acc,2} = \min \left[1, \exp \left((2\tau_x - 1)\tilde{D} \right) \right] . \quad (16)$$

Detailed balance can be easily proven by going through the four cases which are given by positive or negative arguments of the exponential function in Eqs. (15,16). We take two uncorrelated random numbers r_1 and r_2 from a uniform distribution in $[0, 1]$. If both $P_{acc,1} \geq r_1$ and $P_{acc,2} \geq r_2$ the proposal is accepted.

In the first stage of our study, we have used the same random number sequence for all $N_{bit} = 64$ systems that we have simulated in parallel. In the second stage of the study, we have used a modified sequence of the random numbers for the acceptance step (13). We have used a 64 bit integer random number in addition to the random number r that is uniformly distributed in $[0, 1]$. If the i^{th} bit of this integer random number is 1 we take r itself for the acceptance step of the i^{th} system. Otherwise, if the bit is 0, we take $1 - r$ instead. This modification considerably reduces the correlation among the $N_{bit} = 64$ systems that are simulated in parallel.

We have compared the performance of this local update with that of a local heat bath using a standard implementation. To this end, we have simulated a 16^3 lattice at $\beta = 0.3877218$, which is close to β_c as we shall see below. The integrated autocorrelation times in units of sweeps of the energy density and the magnetic susceptibility are by a factor of about 1.3 larger for the Metropolis update discussed here than for the heat bath update. One sweep over $N_{bit} = 64$ systems in parallel using the multispin coding technique takes about 4 times as much CPU-time as one sweep over a single system using the standard implementation of the heat-bath update. In order to compare the efficiency of the two local updates, we have computed the statistical error of the energy and the magnetic susceptibility, taking into account the possible correlation among the $N_{bit} = 64$ systems in the case of the multispin coding implementation. To this end we have performed a Jackknife analysis, where we have first averaged the measurements of the $N_{bit} = 64$ systems at a given iteration of the Monte Carlo simulation. Taking the inverse of the statistical error squared times the CPU time needed as measure of the efficiency, we find a performance gain of a factor of about 10 of the multispin coding implementation of the local Metropolis update compared with the standard implementation of the heat bath update.

During the simulation, local Metropolis sweeps, single cluster and wall cluster updates are performed in a certain sequence. In the following we denote an elementary building block of the sequence by cycle. In the case of our most recent simulations ($D = 0.655$) such a cycle is composed of

- $4 \times$ (2 Metropolis sweeps followed by $L/16$ single cluster updates)
- 3 Metropolis sweeps
- one wall-cluster update

In the case of the wall-cluster update we chose the wall to be perpendicular to the 0, 1 and 2-axis in three subsequent cycles. The position of the wall along the axis is chosen randomly each time. The parameters of the cycle are chosen such that roughly the same amount of CPU-time is spent in each of its three components.

In order to study the performance of the algorithm, we have performed preliminary simulations for $D = 0.655$, where we have determined the autocorrelation function $\rho(t)$ of the magnetic susceptibility and the energy density. The statistics of these runs is 300000 update-cycles for the lattice sizes $L = 16, 32, 64$, and 128 and 82000 update-cycles for $L = 256$ at $\beta = 0.3877218$, which is close to our final estimate of β_c . The integrated autocorrelation time is given by

$$\tau = \frac{1}{2} + \sum_{t=1}^{t_{max}} \rho(t) \quad , \quad (17)$$

where we have chosen $t_{max} = 6\tau$, selfconsistently. Fitting our results for integrated autocorrelation times in units of update-cycles we get

$$\tau_\chi = 0.70(4) \times L^{0.34(1)} \quad (18)$$

for the magnetic susceptibility and

$$\tau_E = 0.47(2) \times L^{0.42(1)} \quad (19)$$

for the energy density. This means that the autocorrelation times are only a few cycles, even for our largest lattices.

We have estimated the statistical errors of the observables using the Jackknife method. As input of this analysis we have taken data that are already averaged over the $N_{bit} = 64$ systems that are simulated in parallel and might be correlated by the use of a common sequence of random numbers during the Metropolis updates. Therefore the possible correlation among these $N_{bit} = 64$ systems does not affect the correctness of the estimate of the statistical errors.

To figure out how much this correlation does affect the efficiency of the algorithm, we have computed the statistical error, taking only one system, and for comparison, averaging over all N_{bit} systems. If the simulations were independent, the square of the ratio of these errors, denoted by R^2 in the following, would be equal to N_{bit} . In fact we see some performance loss due to the use of a common random number sequence. For $L = 16$ we get for the energy density $R^2 \approx 28.6$ and for the magnetic susceptibility $R^2 \approx 36.2$. Fortunately these numbers increase with increasing lattice size. For $L = 256$ we get for the energy density $R^2 \approx 42.2$ and $R^2 \approx 48.8$ for the magnetic susceptibility.

In order to give an accurate result for the performance gain that is achieved by using our particular multispin coding implementation of the local update, one would have to tune the parameters of the update cycle for both types of the local update. For lack of time this could not be done. Since the local update is only one of the three components of the complete update cycle, likely the gain is moderate, certainly less than a factor of two.

A. The simulations: CPU time and statistics

In a first stage of the study we have simulated the spin-1/2 Ising model and the Blume-Capel model at $D = 0.641, \ln 2, 1.15$ and 1.5 . Note that $D = 0.641$ is the estimate of ref. [34] for D^* and $D = \ln 2$ has been simulated before by the authors of refs. [27, 35]. At $D = 1.15$ the amplitude of leading corrections to scaling has about the same magnitude as for the spin-1/2 Ising model but opposite sign. A preliminary analysis of these data resulted in $D^* \approx 0.655$. Therefore we have simulated at $D = 0.655$ in a second stage of our study.

We have simulated lattices of a linear size L up to $L_{max} = 96, 200, 360, 300, 64$ and 48 for the spin-1/2 Ising model and the Blume-Capel model at $D = 0.641, 0.655, \ln 2, 1.15$ and 1.5 , respectively. In table III we have summarized in detail the lattice sizes that we have simulated and the statistics of these simulations.

In total we have spent the equivalent of 3.5, 9, 16, 3, 3, 0.1 CPU years on a single core of a Quad-Core AMD Opteron(tm) Processor 2378 running at 2.4 GHz for the spin-1/2 Ising model and the Blume-Capel model at $D = 0.641, 0.655, \ln 2, 1.15$ and 1.5 , respectively.

As random number generator we have used the SIMD-oriented Fast Mersenne Twister algorithm [43]. As a check we have repeated our simulations at $D = 0.655$ using the WELL Random number generator [44] with about one third of the statistics reported in table III. In particular we have used the program “WELL44497a.c” provided by the authors. We found that the estimates of individual observables are consistent. We have also repeated part of the finite size scaling analysis using these data. For given ansätze we found consistent, even though less precise results for the critical exponents. One should note that the statistical error of the fit parameters is often much smaller than the final error that also includes systematical errors due to subleading corrections. The following analysis is only based on the simulations using the Mersenne Twister algorithm [43].

V. β_c AND THE FIXED POINT VALUES OF PHENOMENOLOGICAL COUPLINGS

In a first step of the analysis we have studied the finite size scaling behavior of the phenomenological couplings at $D = 0.655$, since here we have accumulated the best statistics and secondly, as we shall see below, this value of D is closest to D^* among the values that we have simulated.

At the critical point a phenomenological coupling behaves as

$$R(L, \beta_c) = R^* + aL^{-\omega} + bL^{-\omega'} + cL^{-2\omega} + \dots, \quad (20)$$

where $\omega \approx 0.8$ as discussed in the introduction. Below we shall find $\omega = 0.832(6)$. The subleading corrections exponent is $\omega' = 1.67(11)$ [45]. Furthermore, there should be corrections with $\omega'' \approx 2$ due to the breaking of the rotational symmetry by the lattice [46] or due to the analytic background of the magnetic susceptibility. Motivated by eq. (20), we have fitted our data with three different ansätze

$$R(L, \beta_c) = R^* \quad (21)$$

$$R(L, \beta_c) = R^* + aL^{-\epsilon_1} \quad (22)$$

$$R(L, \beta_c) = R^* + aL^{-\epsilon_1} + bL^{-\epsilon_2}, \quad (23)$$

TABLE III. We give the number of update-cycles divided by 64×15000 as a function of the lattice size and the value of the parameter D . For a discussion see the text.

| L | Ising | 0.641 | 0.655 | $\ln 2$ | 1.15 | 1.5 |
|-----|-------|-------|-------|---------|-------|------|
| 10 | 10000 | 10000 | 4005 | | 10000 | |
| 11 | | | 4005 | | | |
| 12 | 9593 | 20000 | 4000 | 4083 | 10000 | 1000 |
| 13 | | | 4005 | | | |
| 14 | 11747 | 10000 | 4005 | 3003 | 10000 | |
| 15 | | | 3994 | | | |
| 16 | 9740 | 20200 | 3999 | 2371 | 9917 | 1000 |
| 17 | | | 4000 | | | |
| 18 | 11524 | 10000 | 3993 | 1807 | 11102 | |
| 20 | 6959 | 12000 | 3995 | 1828 | 7208 | |
| 22 | 11320 | | 4003 | 1813 | 12328 | |
| 24 | 12000 | 10971 | 4000 | 2471 | 13239 | 1000 |
| 28 | 4374 | 7024 | 3999 | 2920 | 5420 | |
| 32 | 5091 | 2291 | 3011 | 2533 | 4582 | 692 |
| 36 | 3951 | 3362 | | | 3444 | |
| 40 | 1658 | 2349 | 1657 | 1466 | 1474 | |
| 48 | 1890 | 2202 | | | 1502 | 206 |
| 50 | | | 968 | 624 | | |
| 56 | 629 | 824 | | | 688 | |
| 64 | 719 | 697 | 286 | | 485 | |
| 70 | | | 894 | | | |
| 72 | | 848 | | | | |
| 80 | | 1053 | | | | |
| 96 | 273 | | | | | |
| 100 | | 753 | 435 | | | |
| 128 | | | 136 | | | |
| 150 | | 319 | 179 | | | |
| 200 | | 149 | 106 | | | |
| 250 | | | 118 | 58 | | |
| 300 | | | 62 | 14 | | |
| 360 | | | 11 | | | |

where we have used in eq. (22) the choices $\epsilon_1 = 0.83$, $\epsilon_1 = 1.6$ or $\epsilon_1 = 2$ and in eq. (23) $\epsilon_1 = 0.83$ and $\epsilon_2 = 1.6$ or $\epsilon_2 = 2$. Here and in the following ansätze, we denote a correction exponent with a fixed value by ϵ . Instead, if it is a free parameter we shall denote it, as usual, by ω . Here we need the phenomenological couplings R as a function of the inverse temperature. To this end we have used the Taylor-expansion around the value β_s of the inverse temperature that we have used in the simulation. We have checked that the result

TABLE IV. *Fitting the data for Z_a/Z_p obtained at $D = 0.655$ with the ansätze (21,22,23). L_{min} is the minimal lattice size that is included into the fit. For a discussion see the text.*

| ansatz | ϵ_1 | ϵ_2 | L_{min} | β_c | $(Z_a/Z_p)^*$ | $\chi^2/\text{d.o.f.}$ |
|--------|--------------|--------------|-----------|-----------------|---------------|------------------------|
| 21 | - | - | 32 | 0.387721745(10) | 0.542489(14) | 9.5/10 |
| 22 | 0.83 | - | 18 | 0.387721730(12) | 0.542589(33) | 12.4/14 |
| 22 | 1.6 | - | 12 | 0.387721729(10) | 0.542558(12) | 24.0/20 |
| 22 | 2 | - | 10 | 0.387721734(10) | 0.542532(8) | 27.4/22 |
| 23 | 0.83 | 1.6 | 10 | 0.387721746(12) | 0.542448(46) | 27.6/21 |
| 23 | 0.83 | 2 | 10 | 0.387721740(12) | 0.542502(38) | 26.8/21 |

TABLE V. *Results for the inverse critical temperature β_c at $D = 0.655$ obtained from the FSS study of various phenomenological couplings. In addition we give the fixed point values R^* of these quantities. For a discussion see the text.*

| | Z_a/Z_p | ξ_{2nd}/L | U_4 | U_6 |
|-----------|---------------|---------------|---------------|---------------|
| β_c | 0.38772174(2) | 0.38772174(2) | 0.38772173(2) | 0.38772173(2) |
| R^* | 0.5425(1) | 0.6431(1) | 1.6036(1) | 3.1053(5) |

for β_c and β_s are sufficiently close to avoid significant truncation effects. This way, for example eq. (21) becomes

$$R(L, \beta_s) = R^* - c_1(L, \beta_s)(\beta_c - \beta_s) - \frac{c_2(L, \beta_s)}{2!}(\beta_c - \beta_s)^2 - \frac{c_3(L, \beta_s)}{3!}(\beta_c - \beta_s)^3, \quad (24)$$

where R^* and β_c are the two parameters of the fit. Since we have chosen β_s as a good approximation of β_c , we could ignore the relatively small statistical error of the Taylor coefficients c_1 , c_2 and c_3 , which simplifies the fit.

As an example let us discuss the results obtained for Z_a/Z_p in more detail. A selection of our results is given in table IV. We have fitted the data for all linear lattice sizes L that are larger than or equal to a certain L_{min} . Starting from the L_{min} given in column 5 of table IV the $\chi^2/\text{d.o.f.}$ is close to one.

Taking into account the variation of the results over the different ansätze we arrive at our final estimate $\beta_c = 0.38772174(2)$ and $(Z_a/Z_p)^* = 0.5425(1)$. We performed a similar analysis for ξ_{2nd}/L , U_4 and U_6 . Our final results are summarized in table V. We find that the estimates of β_c obtained from different phenomenological couplings are consistent within error bars. We take the average

$$\beta_c = 0.387721735(25) \quad (25)$$

as our final estimate of the inverse critical temperature. The error bar is chosen such that it covers all results given in table V, including their error bars.

Our result for U_4^* is about 3 times the combined error smaller than $U_4^* = 1/0.62341(4) = 1.60408(10)$ given in [27]. We regard our result as more reliable, since we have simulated

TABLE VI. *Estimates of the inverse critical temperature β_c of the spin-1/2 Ising model and the Blume-Capel model at various values of D . For a discussion see the text.*

| D | β_c |
|---------------------------|-----------------|
| Ising | 0.22165463(8) |
| 0.641 | 0.38567122(5) |
| 0.655 | 0.387721735(25) |
| $\ln 2 = 0.69314718\dots$ | 0.39342239(8) |
| 1.15 | 0.4756110(2) |
| 1.5 | 0.5575303(10) |

larger lattices and have carefully estimated systematic errors due to subleading corrections that are not included into the fit.

In the case of the other models we also determined β_c by fitting with the ansätze (21,22,23). Here however we have used the results for $(Z_a/Z_p)^*$, $(\xi_{2nd}/L)^*$, U_4^* and U_6^* given in table V as input. The final results obtained this way are summarized in table VI. For completeness we have included the results for $D = 0.655$ given in eq. (25).

Our result for β_c of the spin-1/2 Ising model is fully consistent with $\beta_c = 0.22165455(3)$ given in [27]. For a summary of previous results for β_c of the spin-1/2 Ising model we refer the reader to table 1 of [34]. Our result for β_c at $D = \ln 2$ is by 1.5 times the combined error larger than $\beta_c = 0.39342225(5)$ given in [27].

VI. THE CORRECTION EXPONENT ω AND THE IMPROVED MODEL

In this section we study the cumulants U_4 and U_6 at a fixed value of Z_a/Z_p or ξ_{2nd}/L . To this end one determines the inverse temperature $\beta_f(L)$ defined by

$$R_1(L, \beta_f(L)) = R_{1,f} \quad , \quad (26)$$

where R_1 is either Z_a/Z_p or ξ_{2nd}/L and $R_{f,1}$ the required value. As $R_{f,1}$ we take the fixed point values of Z_a/Z_p and ξ_{2nd}/L obtained above. We define

$$\bar{R}_2(L) \equiv R_2(L, \beta_f(L)) \quad , \quad (27)$$

where R_2 is, in our case, either U_4 or U_6 . In the following we shall denote \bar{R}_2 by R_2 at $R_1 = R_{1,f}$. In practice we have done these calculations using the Taylor-expansion of R_1 and R_2 around the value β_s that we have used in the simulation up to third order. We have checked carefully that β_s and β_f are sufficiently close to avoid significant truncation errors.

One finds, see e.g. section III of [37]

$$\bar{R}(D, L) = \bar{R}^* + a(D)L^{-\omega} + b(D)L^{-\omega'} + \dots + c a^2(D)L^{-2\omega} + \dots \quad , \quad (28)$$

where we should note that the correction amplitudes depend on the parameter D of our model. The improved model is characterized by a vanishing amplitude of leading

corrections to scaling. Hence D^* is given by the zero of $a(D)$. We have analyzed the data of 5 different models in combined fits: The Ising model and the Blume-Capel model at $D = 0.641$, $D = 0.655$, $D = \ln 2$ and $D = 1.15$. To this end we have employed various ansätze that are derived from eq. (28):

$$\bar{R}(D, L) = \bar{R}^* + a(D)L^{-\omega} \quad (29)$$

$$\bar{R}(D, L) = \bar{R}^* + a(D)L^{-\omega} + c a^2(D)L^{-2\omega} \quad (30)$$

$$\bar{R}(D, L) = \bar{R}^* + a(D)L^{-\omega} + c a^2(D)L^{-2\omega} + bL^{-\epsilon} \quad (31)$$

$$\bar{R}(D, L) = \bar{R}^* + a(D)L^{-\omega} + c a^2(D)L^{-2\omega} + d a^3(D)L^{-3\omega} \quad (32)$$

$$\bar{R}(D, L) = \bar{R}^* + a(D)L^{-\omega} + c a^2(D)L^{-2\omega} + d a^3(D)L^{-3\omega} + bL^{-\epsilon} . \quad (33)$$

In the ansatz (29) the free parameters of the fit are \bar{R}^* , $a(\text{Ising})$, $a(0.641)$, $a(0.655)$, $a(\ln 2)$, $a(1.15)$ and the correction exponent ω . In the ansatz (30) we have in addition the parameter c . In the ansatz (31) we have added the term $bL^{-\epsilon}$ to take subleading corrections into account. Here we make the approximation that the parameter b is model independent. We fix the subleading correction exponent $\epsilon = 1.6$ or $\epsilon = 2$. In the ansatz (32) we take into account corrections $\propto L^{-3\omega}$. Finally in the ansatz (33) we add, similar to eq. (31) a term $bL^{-\epsilon}$.

In the case of the ansatz (29) fits with $\chi^2/\text{d.o.f.} < 2$ are only obtained for $L_{\min} \geq 36$. Instead, fitting with ansatz (30) we get for U_4 at $Z_a/Z_p = 0.5425$ $\chi^2/\text{d.o.f.} = 62.4/62$ already for $L_{\min} = 16$. The results for the parameters of this fit are $\omega = 0.832(1)$, $\bar{U}_4^* = 1.60357(1)$, $a(\text{Ising}) = -0.2983(6)$, $a(0.641) = -0.0067(2)$, $a(0.655) = -0.0006(2)$, $a(\ln 2) = 0.0167(2)$, $a(1.15) = 0.380(1)$, and $c = 2.08(3)$. Note that here and in the following the errors quoted for results of individual fits are purely statistical. Extrapolating $a(0.641)$ and $a(0.655)$ we get $D^* = 0.6564(5)$.

We estimated the systematic error due to corrections that are not taken into account in the ansatz (30) from the variation of the results obtained with the ansätze (31,32,33) and by using U_6 instead of U_4 . Furthermore we have redone the analysis for U_4 and U_6 at $\xi_{2nd}/L = 0.6431$. We arrive at the final estimates

$$\omega = 0.832(6) \quad (34)$$

$$D^* = 0.656(20) . \quad (35)$$

It also follows from the fits that the amplitude of corrections to scaling at $D = 0.655$ is at least by a factor of 30 smaller than that of the spin-1/2 Ising model.

VII. IMPROVED OBSERVABLES

The exponent ν can be obtained from the behavior of the slope of a phenomenological coupling at the critical point:

$$\left. \frac{\partial R}{\partial \beta} \right|_{\beta=\beta_c} = aL^{1/\nu} (1 + bL^{-\omega} + \dots) . \quad (36)$$

The exponent η can be extracted from the behavior of the magnetic susceptibility at the critical point:

$$\chi|_{\beta=\beta_c} = aL^{2-\eta} (1 + bL^{-\omega} + \dots) . \quad (37)$$

Note that the coefficients a and b of course take different values in eq. (36) and eq. (37). Such a procedure requires an estimate of β_c . To avoid this we have studied, following [25], the slopes and the magnetic susceptibility at β_f as defined in eq. (26). These quantities behave as

$$\overline{\frac{\partial R}{\partial \beta}} \equiv \left. \frac{\partial R}{\partial \beta} \right|_{\beta=\beta_f} = a(D)L^{1/\nu} (1 + b(D)L^{-\omega} + \dots) \quad (38)$$

and

$$\bar{\chi} \equiv \chi|_{\beta=\beta_f} = a(D)L^{2-\eta} (1 + b(D)L^{-\omega} + \dots) \quad (39)$$

Again we have computed these quantities using their Taylor-expansion around β_s up to the third order.

Here, following [28], we shall study improved versions of the slopes and the magnetic susceptibility. This means in the ideal case that the amplitude of leading corrections vanishes for any model. In practice, as we shall see below, we can construct quantities for that the amplitude of leading corrections is suppressed by more than one order of magnitude. Using such quantities in the case of improved models ensures that leading corrections to scaling are suppressed by two to three orders of magnitude compared with standard observables in the case of e.g. the spin-1/2 Ising model. This is sufficient to ignore leading corrections to scaling in the analysis of our data.

Let us discuss in detail the construction of the improved observable at the example of the magnetic susceptibility. We consider

$$\bar{\chi}_{imp}(L, D) = \bar{U}_4(L, D)^x \bar{\chi}(L, D) \quad , \quad (40)$$

where x is chosen such that the amplitude of leading corrections vanishes. Note that instead of \bar{U}_4 also \bar{U}_6 could be used. It is important to take a phenomenological coupling, where leading corrections to scaling are clearly visible. Let us recall the finite size scaling behavior of the Binder cumulant

$$\bar{U}_4(L, D) = \bar{U}_4^* + b_U(D)L^{-\omega} + \dots \quad (41)$$

Inserting eq. (39) and eq. (41) into eq. (40) we get

$$\bar{\chi}_{imp}(L, D) = a(D)\bar{U}_4^x L^{2-\eta} \left(1 + \left[b(D) + x \frac{b_U(D)}{\bar{U}_4^*} \right] L^{-\omega} + \dots \right) \quad (42)$$

Hence the exponent defining the improved observable is given by

$$x = -b(D) \frac{\bar{U}_4^*}{b_U(D)} \quad (43)$$

Note that ratios of correction amplitudes are universal. Therefore the exponent x does not depend on D . It can be best determined by analyzing data obtained for models with relatively large corrections to scaling. For example one might consider the spin-1/2 Ising model to this end. We have already determined $b_U(\text{Ising})$ and \bar{U}_4^* in the previous section. In order to obtain $b(D)$ one would fit $\bar{\chi}(L, D)$ with ansätze motivated by eq. (39).

However it turns out to be more efficient to study ratios of observables taken from two different models. This way, critical exponents cancel and therefore fits have less

parameters and become more reliable. In particular we shall study the spin-1/2 Ising model and the Blume-Capel at $D = 1.15$. We define

$$R_\chi(L) = \frac{\bar{\chi}(L, \text{Ising})}{\bar{\chi}(L, D = 1.15)} = \frac{a(\text{Ising})}{a(D = 1.15)} (1 + [b(\text{Ising}) - b(1.15)]L^{-\omega} + \dots) \quad (44)$$

and

$$R_U(L) = \frac{\bar{U}(L, \text{Ising})}{\bar{U}(L, D = 1.15)} = 1 + \frac{b_U(\text{Ising}) - b_U(1.15)}{\bar{U}^*} L^{-\omega} + \dots, \quad (45)$$

where now

$$x = -[b(\text{Ising}) - b(1.15)] \frac{\bar{U}^*}{b_U(\text{Ising}) - b_U(1.15)}. \quad (46)$$

The exponent x can be directly obtained from fits with the ansatz

$$R_U(L)^x R_\chi(L) = C, \quad (47)$$

where x and C are the parameters of the fit. To check for the effect of subleading corrections we have also fitted the data with the ansatz

$$R_U(L)^x R_\chi(L) = C + cL^{-\epsilon}, \quad (48)$$

where c is an additional parameter and we have fixed either $\epsilon = 1.6$ or $\epsilon = 2$. Fixing $Z_a/Z_p = 0.5425$, fits with the ansatz (47) have an $\chi^2/\text{d.o.f.} \approx 1$ starting with $L_{\min} = 16$. Using $L_{\min} = 16$ we get $x = -0.656(1)$. Instead using the ansatz (48) we get $\chi^2/\text{d.o.f.} \approx 1$ already for $L_{\min} = 10$. The results for $L_{\min} = 10$ are $x = -0.665(2)$ and $x = -0.661(2)$ for $\epsilon = 1.6$ and $\epsilon = 2$, respectively. As our final result we quote $x = -0.66(1)$, where the error is chosen such that it covers the three estimates given above. In a similar fashion we arrive at $x = -0.57(2)$ for fixing $\xi_{2nd}/L = 0.6431$.

In figure 1 we demonstrate the effectiveness of the improvement. We have analyzed our data for χ at $Z_a/Z_p = 0.5425$ for the Ising model and the Blume-Capel model at $D = 1.15$. To this end, we have fitted our data with the ansatz

$$\bar{\chi} = aL^{2-\eta} + B, \quad (49)$$

where B is an analytic background. Using the standard magnetic susceptibility, we get $\chi^2/\text{d.o.f.} = 4.6/4$ for $L_{\min} = 32$ in the case of the Ising model and $\chi^2/\text{d.o.f.} = 2.6/5$ for $L_{\min} = 24$ in the case of the Blume-Capel model at $D = 1.15$. Nevertheless for e.g. $L_{\min} = 32$ the results for η obtained from the two different models differ by more than 20 standard deviations. In contrast, for the improved magnetic susceptibility the results obtained for the two models are quite similar. In particular for $L_{\min} = 24$ the estimates for η obtained from the Ising model and the Blume-Capel model at $D = 1.15$ are consistent within the error bars.

We also have constructed improved slopes

$$\bar{S}_{\text{imp}}(L, D) = \bar{U}_4(L, D)^x \bar{S}(L, D), \quad (50)$$

where x is chosen such that leading corrections to scaling vanish. We have determined x analogous to the case of the magnetic susceptibility discussed above. To this end we have computed the ratios

$$R_S(L) = \frac{\bar{S}(L, \text{Ising})}{\bar{S}(L, D = 1.15)}. \quad (51)$$

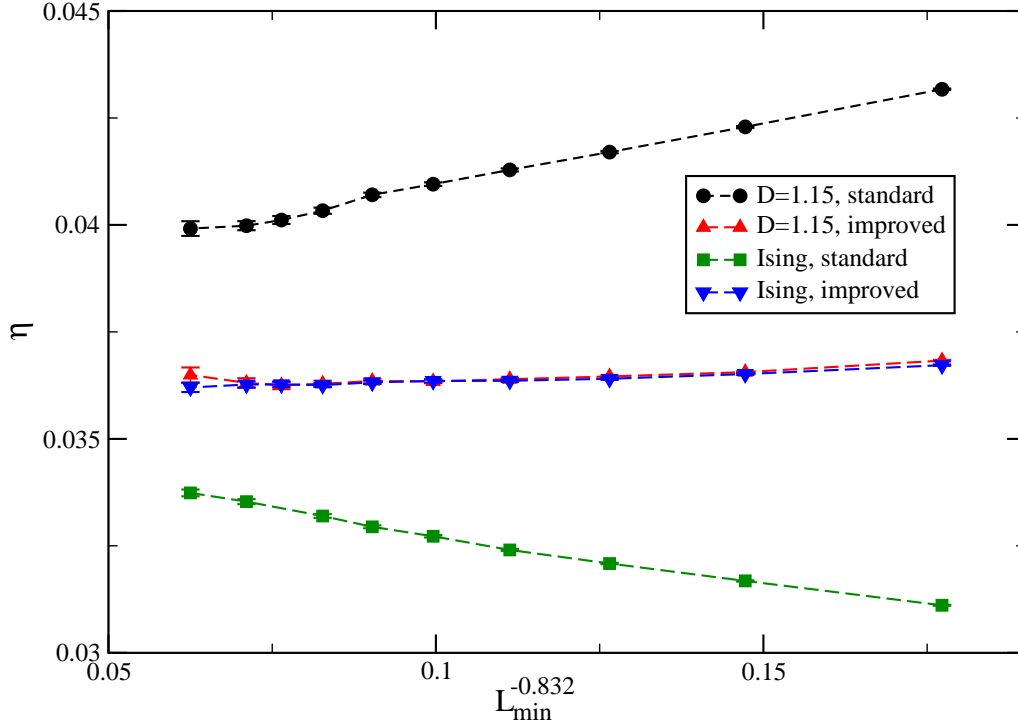


FIG. 1. Results for the critical exponent η obtained by fitting the standard and the improved magnetic susceptibility at $Z_a/Z_p = 0.5425$ for the Ising model and the Blume-Capel model at $D = 1.15$ using the ansatz (49). L_{min} is the minimal lattice size that is taken into account. In the case of the improved magnetic susceptibility, the results obtained from the two different models fall nicely on top of each other. The dashed lines should only guide the eye.

TABLE VII. Exponent x of improved slopes as defined by eq. (50). In the first column we give the phenomenological coupling and its value that is used to define β_f . In the first row we give the quantity whose slope is considered. For a discussion see the text.

| fix ; slope of | Z_a/Z_p | ξ_{2nd}/L | U_4 | U_6 |
|------------------------|-----------|---------------|----------|----------|
| $Z_a/Z_p = 0.5425$ | 0.52(2) | 0.77(3) | -1.21(5) | -2.73(5) |
| $\xi_{2nd}/L = 0.6431$ | 0.54(2) | 0.81(2) | -1.21(3) | -2.71(4) |

As discussed above for the case of the magnetic susceptibility, we have fitted

$$R_U(L)^x R_S(L) = C \quad (52)$$

with x and C as free parameters and, as check

$$R_U(L)^x R_S(L) = C + cL^{-\epsilon} \quad , \quad (53)$$

where c is an additional parameter and ϵ is fixed to either 1.6 or 2. Our final results for the exponent x are summarized in table VII.

TABLE VIII. Exponent x of improved slopes as defined by eq. (54). In the first column we give the phenomenological coupling and its value that is used to define β_f . In the first row we give the quantity whose slope is mixed with that of \bar{U}_4 . For a discussion see the text.

| fix ; slope of | Z_a/Z_p | ξ_{2nd}/L |
|------------------------|-----------|---------------|
| $Z_a/Z_p = 0.5425$ | 0.29(1) | 0.39(1) |
| $\xi_{2nd}/L = 0.6431$ | 0.31(1) | 0.41(1) |

Furthermore we have constructed quantities of the type

$$\bar{S}_{ij} = |\bar{S}_i|^x |\bar{S}_j|^{1-x} , \quad (54)$$

where x is again chosen such that the amplitude of the leading correction vanishes. Here we performed fits with the ansatz

$$R_{S_i}^x R_{S_j}^{1-x} = C , \quad (55)$$

where x and C are the parameters of the fit and

$$R_{S_i}^x R_{S_j}^{1-x} = C + cL^{-\epsilon} \quad (56)$$

with the additional parameter c . Also here we have fixed either $\epsilon = 1.6$ or $\epsilon = 2$. In practice we have combined the slope of U_4 with the slope of Z_a/Z_p or ξ_{2nd}/L . Our results for the exponent x are summarized in table VIII. Notice that the results obtained for $Z_a/Z_p = 0.5425$ and $\xi_{2nd}/L = 0.6431$ are similar but not identical.

VIII. THE EXPONENT η

We have fitted our data for the improved magnetic susceptibility at $Z_a/Z_p = 0.5425$ and $\xi_{2nd}/L = 0.6431$ using the ansätze

$$\bar{\chi}_{imp} = a(D)L^{2-\eta} \quad (57)$$

$$\bar{\chi}_{imp} = a(D)L^{2-\eta} + B(D) \quad (58)$$

$$\bar{\chi}_{imp} = a(D)L^{2-\eta} (1 + d(D)L^{-\epsilon}) . \quad (59)$$

In the ansatz (58) we have taken into account the analytic background B of the magnetic susceptibility. Since η is small, the parameter B also takes effectively into account other corrections that have a correction exponent $\omega'' \approx 2$ like for example the breaking of the rotational symmetry by the lattice. In the ansatz (59) we have set $\epsilon = 1.6$. Using this ansatz we try to estimate the possible effect of a correction caused by $\omega' = 1.67(11)$ [45] on our estimate of η .

We have fitted the data for $D = 0.641$ and $D = 0.655$ in a common fit. The parameters of these fits are $a(0.641)$, $a(0.655)$ and η in the case of the ansatz (57) and in addition $B(0.641)$ and $B(0.655)$ or $d(0.641)$ and $d(0.655)$ in the case of the ansatz (58) or (59), respectively. In figure 2 we have plotted estimates of η obtained by fitting with the ansatz (57) as a function of L_{min}^{-2} . Up to $L_{min} = 48$ the results fall roughly on a straight

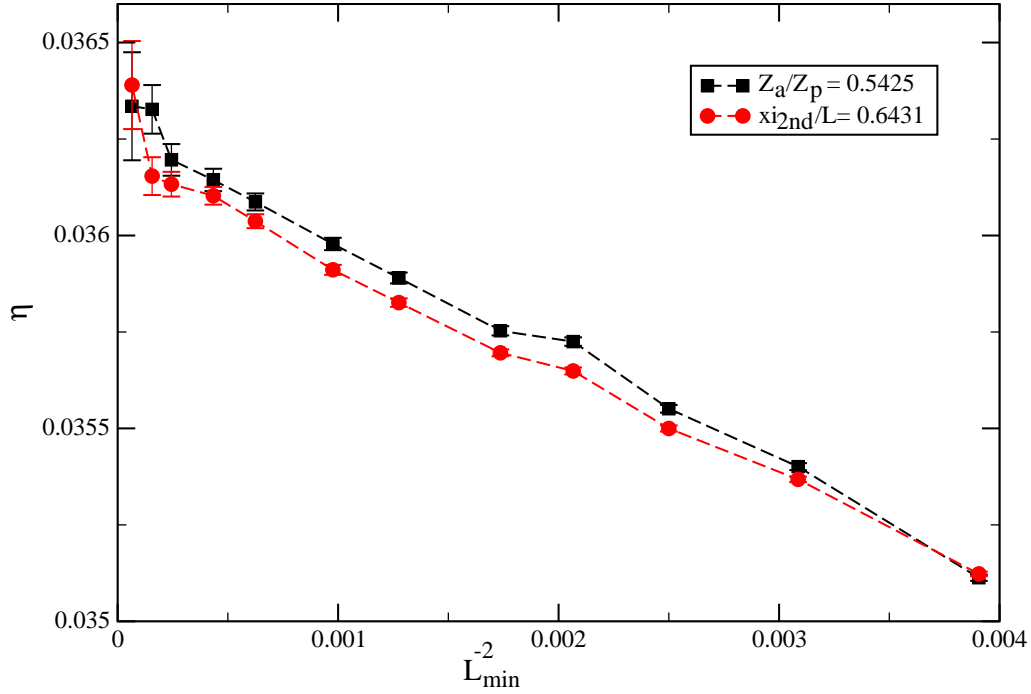


FIG. 2. Results for the critical exponent η obtained by fitting the improved magnetic susceptibility at $Z_a/Z_p = 0.5425$ and at $\xi_{2nd}/L = 0.6431$ using the ansatz (57). Data for the Blume-Capel model at $D = 0.641$ and $D = 0.655$ are taken into account. L_{min} is the minimal lattice size that is taken into account. The dashed lines should only guide the eye. For a discussion see the text.

line, indicating that corrections with an exponent $\epsilon \approx 2$ are present. For $L_{min} = 128$ one finds that $\chi^2/\text{d.o.f.}$ is smaller than one for both taking the improved susceptibility at $Z_a/Z_p = 0.5425$ and $\xi_{2nd}/L = 0.6431$. The estimate $\eta = 0.03636(20)$ covers both results obtained at $L_{min} = 128$, including their error bars.

Next we have fitted our data with the ansatz (58). For both the improved magnetic susceptibility at $\xi_{2nd} = 0.6431$ and at $Z_a/Z_p = 0.5425$ we get $\chi^2/\text{d.o.f.} < 2$ starting from $L_{min} = 14$. The results for η are plotted in figure 3. In the case of $\xi_{2nd} = 0.6431$ the estimate of η is increasing with increasing L_{min} , while it is decreasing for $Z_a/Z_p = 0.5425$. For $L_{min} = 32$ the two results are consistent within error bars.

We read off our final estimate

$$\eta = 0.03627(10) . \quad (60)$$

The error estimate is chosen such that it also covers results obtained with the ansatz (59) and $L_{min} = 32$.

IX. THE CRITICAL EXPONENT ν

In order to determine the exponent ν we performed combined fits of our data for the improved slopes at $D = 0.641$ and $D = 0.655$. In a first step of the analysis we have fitted the improved slopes with a power law without any correction

$$S = a(D)L^{1/\nu} , \quad (61)$$

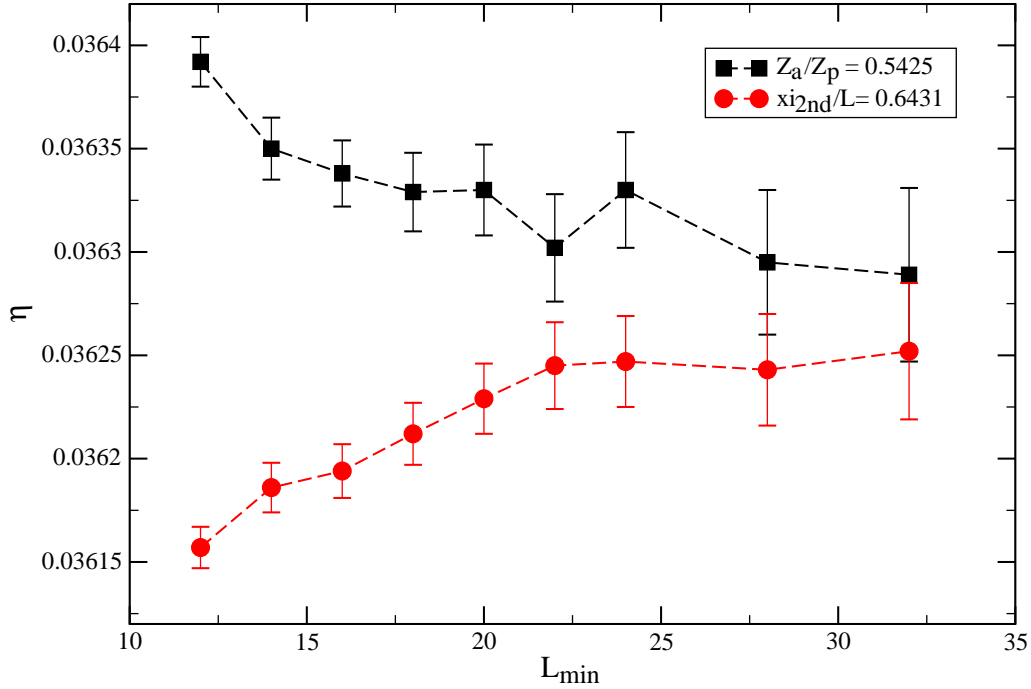


FIG. 3. Results for the critical exponent η obtained by fitting the improved magnetic susceptibility at $Z_a/Z_p = 0.5425$ and at $\xi_{2nd}/L = 0.6431$ using the ansatz (58). Data for the Blume-Capel model at $D = 0.641$ and $D = 0.655$ are taken into account. L_{min} is the minimal lattice size that is taken into account. The dashed lines should only guide the eye. For a discussion see the text.

where the amplitudes $a(0.641)$, $a(0.655)$ and the exponent ν are the parameters of the fit. In figure 4 we give the results for ν as a function of L_{min}^{-2} , where L_{min} is the minimal lattice size that is included into the fit. In the figure we give only results for taking the slopes at $Z_a/Z_p = 0.5425$. Those for the slopes at $\xi_{2nd}/L = 0.6431$ behave in a very similar way.

We find that the result for ν obtained from the improved slope of Z_a/Z_p is increasing with increasing L_{min} , while the one obtained from ξ_{2nd}/L is decreasing. The results obtained from the improved slope of U_4 and U_6 are quite similar. They only slightly increase with increasing L_{min} . We have also plotted results obtained from the combined slopes (54). In the case of combining the slope of U_4 with that of ξ_{2nd}/L the estimate of ν is decreasing with increasing L_{min} , while for combining the slope of U_4 with that of Z_a/Z_p it is increasing. In all cases a rather large L_{min} is needed to get acceptable values for $\chi^2/\text{d.o.f.}$. In the worst case, for the improved slope of Z_a/Z_p only for $L_{min} \geq 56$ a $\chi^2/\text{d.o.f.}$ smaller than two is reached. The behavior of the estimates of ν for $L_{min} < 48$ is consistent with the fact that the dominating corrections have an exponent $\omega' \approx 2$. For larger L_{min} , the variation of our estimates of ν with L_{min} seems to be dominated by statistical fluctuations. For $L_{min} = 128$ we get $\chi^2/\text{d.o.f.}$ smaller than one for all quantities that we have considered. The estimate $\nu = 0.6301(3)$ covers the results, including the statistical error, of all our fits for $L_{min} = 128$. Note that in ref. [27] $L = 128$ is the largest lattice size that is simulated.

Motivated by these observations, we have fitted our data with the ansatz

$$S = a(D)L^{1/\nu} \times (1 + bL^{-\epsilon}) \quad , \quad (62)$$

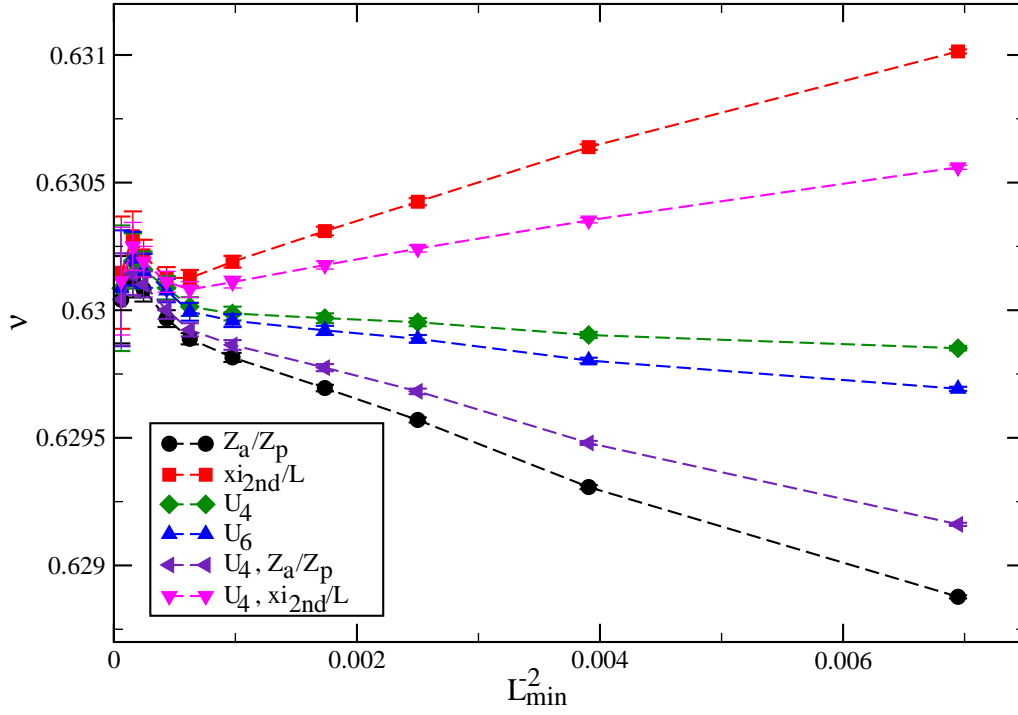


FIG. 4. Results for the critical exponent ν obtained by fitting improved slopes of various phenomenological couplings at $Z_a/Z_p = 0.5425$ as a function of L_{min}^{-2} , where L_{min} is the minimal lattice size that is included into the fit. The dashed lines should only guide the eye. For a discussion see the text.

where we have fixed ϵ to either 1.6 or 2. Since already $a(0.641)$ and $a(0.655)$ are very similar, we have chosen the parameter b to be model independent. Let us first discuss the fits with $\epsilon = 2$. Such fits give $\chi^2/\text{d.o.f.}$ close to one already for $L_{min} = 10$. In the lower part of figure 5 we have plotted the results obtained from the slopes of different quantities for $10 \leq L_{min} \leq 24$. These different estimates of ν are consistent among each other. Furthermore there is little variation of the results with L_{min} .

In the upper part of figure 5 we plot the corresponding result for $\epsilon = 1.6$. Here the $\chi^2/\text{d.o.f.}$ is somewhat larger than for $\epsilon = 2$. Also the result for ν clearly depends on the quantity that is analyzed. We conclude that the numerically dominant corrections have an exponent $\epsilon \approx 2$. Motivated by these fits, we take $\nu = 0.63002$ as our final result. Since we can not exclude that there are also corrections with an exponent $\epsilon \approx 1.6$, we take these fits into account in our final error of ν . For $L_{min} = 22$ and $L_{min} = 24$ all results that we have obtained with the ansatz (62), including their error bar, are contained in the interval $[0.62992, 0.63012]$. Therefore we quote as our final result

$$\nu = 0.63002(10) . \quad (63)$$

X. SUMMARY AND CONCLUSIONS

We have simulated the spin-1/2 Ising model and the Blume-Capel model on the simple cubic lattice using linear lattice sizes $L \leq 360$. Using finite size scaling methods we

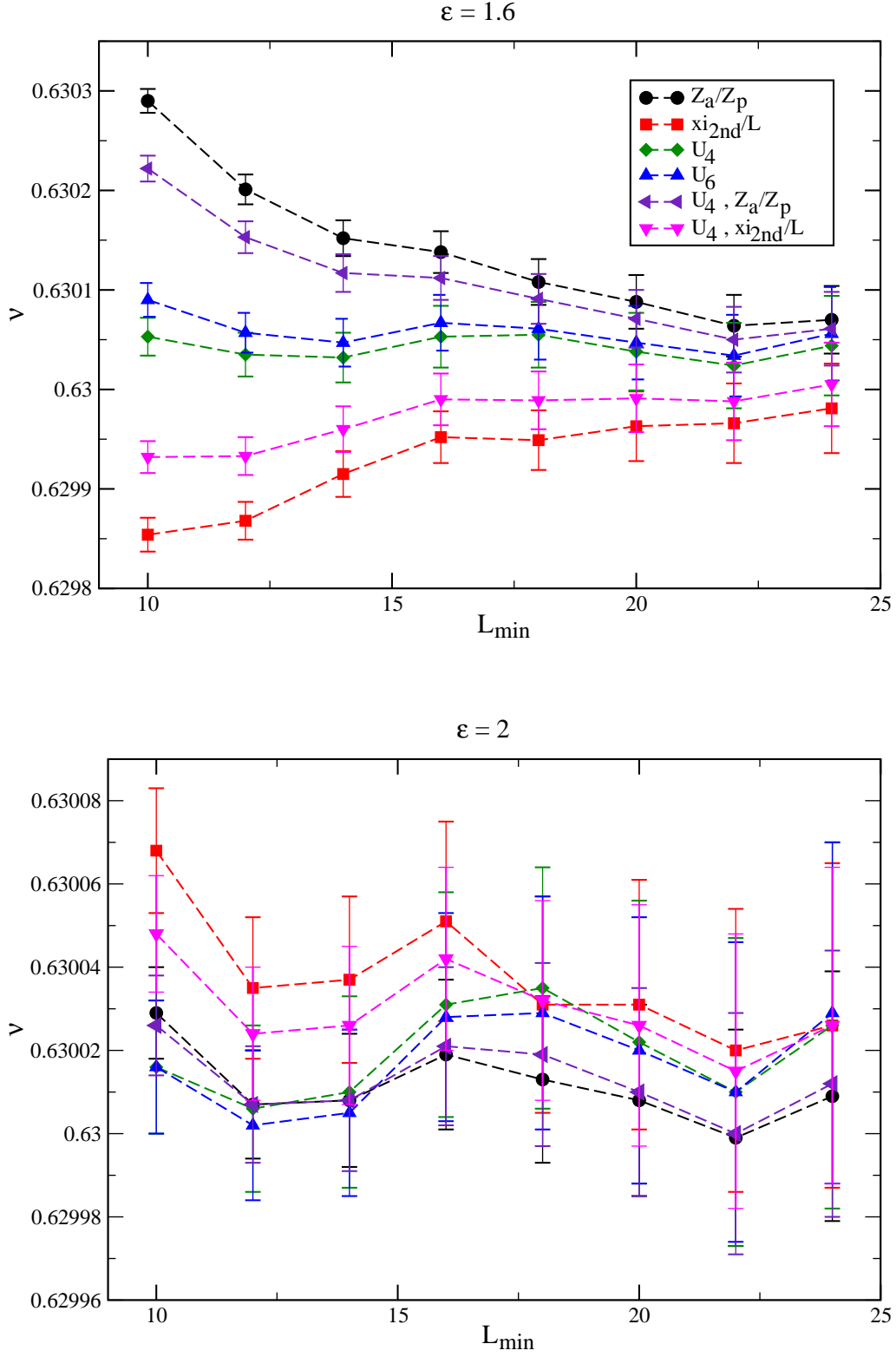


FIG. 5. Results for the critical exponent ν obtained by fitting improved slopes of various phenomenological couplings at $Z_a/Z_p = 0.5425$ with the ansatz (62) as a function of L_{min} . In the upper part of the figure the correction exponent is fixed to $\epsilon = 1.6$ and in the lower part it is fixed to $\epsilon = 2$. The dashed lines should only guide the eye. For a discussion see the text.

have determined critical properties of these models. In particular we have determined the value $D^* = 0.656(20)$ of the parameter D of the Blume-Capel model, where leading corrections to scaling vanish. We have accurately determined the inverse of the critical temperature for various values of D , in particular $\beta_c(0.641) = 0.38567122(5)$ and $\beta_c(0.655) = 0.387721735(25)$. We have computed the critical exponents $\nu = 0.63002(10)$ and $\eta = 0.03627(10)$ as well as the exponent $\omega = 0.832(6)$ of leading corrections to scaling. The errors quoted for these final results cover statistical as well as systematical errors. Systematical errors are due to the fact that power laws like eqs. (36,37) that govern the finite size scaling behavior of physical quantities at the critical temperature are subject to an infinite series of correction terms. Fitting Monte Carlo data, only few of these correction terms can be taken into account. In the present study, we have effectively eliminated the leading correction $\propto L^{-\omega}$ by simulating an improved model and analyzing improved observables as discussed in section VII. In our ansätze we take into account a sub-leading correction with the exponent $\omega' = 1.67(11)$ predicted by [45] or $\omega'' \approx 2$ due to the breaking of the rotational symmetry by the simple cubic lattice [46] or due to the analytic background of the magnetic susceptibility. We estimate the error caused by correction terms that are not included by comparing the results obtained by using different ansätze and, even more important, by fitting different quantities. One expects that in the generic case the amplitudes of corrections are different for different quantities. In the case of the critical exponent ν we have studied the slope of four different phenomenological couplings: The cumulants U_4 and U_6 , the ratio of partition functions Z_a/Z_p , and the second moment correlation length over the linear lattice size ξ_{2nd}/L . We regard the estimates of the error obtained this way as quite robust and therefore the results obtained here should serve well as benchmark for experimental studies as well as new or developing theoretical methods.

Our results are fully consistent with those obtained from high temperature series expansion of lattice models [17–19]; See table II. We find a small discrepancy with the Monte Carlo results of ref. [27]; See table II. Note that the authors of [27] did not take into account a sub-leading correction with the exponent $\omega' = 1.67(11)$ [45] analyzing their Monte Carlo data.

The accuracy that is reached now by lattice methods has clearly outpaced that of field theoretic methods. Furthermore, comparing with the numbers that are summarised in table I, we notice that most of the results for η and ω obtained from the perturbative expansion in three dimensions fixed are at odds with ours, while those of [11, 13] are in reasonable agreement. Note that, as discussed by Nickel [13], the subleading correction exponent $\omega' = 1.67(11)$ [45] also plays a crucial role in the analysis of the perturbative series in three dimensions fixed. Therefore, it would be highly desirable to get an estimate of ω' by using a different method.

Using Monte Carlo simulations, the error of the estimates of the critical exponents can be further reduced just by spending more CPU time. To this end one has to increase the statistics as well as enlarge the size of the lattices that are simulated. Keeping the statistical error and the systematical one proportional, the effort increases as $\text{error}^{-2-(3+z)/\omega'}$ with a decreasing error, where the first factor error^{-2} is related to the increased statistics and the second to the larger linear lattice size L that is needed to reduce the systematical error. Here we assume that the systematical error is proportional to $L^{-\omega'}$, since, as we have shown here, leading corrections can be eliminated. The effort at a fixed statistical accuracy behaves as L^{d+z} , where $d = 3$ is the dimension of the system and z is the critical dynamical exponent. In a recent study of a spin glass [47] about 1000 years of CPU

time on one core of a CPU of similar performance as the one used here had been spent. This is about a factor of 30 more CPU time than we have spent here. One should notice however that this factor in CPU time only would allow to reduce the errors of the critical exponents by a factor of about 2.3, where we have assumed $\omega' \approx 1.6$ and $z \approx 0.4$; see Eqs. (18,19).

XI. ACKNOWLEDGEMENTS

This work was supported by the DFG under the grant No HA 3150/2-1.

-
- [1] K. G. Wilson and J. Kogut, Phys. Rep. C **12**, 75 (1974).
 - [2] M. E. Fisher, Rev. Mod. Phys. **46**, 597 (1974).
 - [3] M. E. Fisher, Rev. Mod. Phys. **70**, 653 (1998).
 - [4] A. Pelissetto and E. Vicari, Phys. Rept. **368**, 549 (2002).
 - [5] J. V. Sengers and J. G. Shanks, J. Stat. Phys. **137** 857 (2009).
 - [6] M. Barmatz, I. Hahn, J. A. Lipa, and R. V. Duncan, Rev. Mod. Phys. **79**, 1 (2007).
 - [7] A. Lytle and D. T. Jacobs, J. Chem. Phys. **120**, 5709 (2004).
 - [8] K. G. Wilson, M. E. Fisher, Phys. Rev. Lett. **28**, 240 (1972).
 - [9] G. Parisi, Cargèse Lectures (1973), J. Stat. Phys. **23**, 49 (1980).
 - [10] K. G. Chetyrkin, S. G. Gorishny, S. A. Larin, and F. V. Tkachov, Phys. Lett. B **132**, 351 (1983); H. Kleinert, J. Neu, V. Schulte-Frohlinde, K. G. Chetyrkin, and S. A. Larin, Phys. Lett. B **272**, 39 (1991), (E) Phys. Lett. B **319**, 545 (1993).
 - [11] D. B. Murray, B. G. Nickel, *Revised estimates for critical exponents for the continuum n-vector model in 3 dimensions*, unpublished Guelph University report (1991). The coefficients of the loop-expansion are reported e.g. in ref. [15]. Numerical results for the critical exponents are reported in table IV of ref. [14]).
 - [12] R. Guida, J. Zinn-Justin, J. Phys. A **31**, 8103 (1998) [arXiv:cond-mat/9803240]
 - [13] B. G. Nickel, Physica A **177**, 189 (1991).
 - [14] H. Kleinert, Phys. Rev. D **60**, 085001 (1999).
 - [15] F. Jasch and H. Kleinert, J. Math. Phys. **42**, 52 (2001) [arXiv:cond-mat/9906246]
 - [16] A. A. Pogorelov and I. M. Suslov, J. of Experimental and Theoretical Physics **106**, 1118 (2008) [arXiv:1010.3389]
 - [17] M. Campostrini, A. Pelissetto, P. Rossi, and E. Vicari, Phys. Rev. E **65**, 066127 (2002) [arXiv:cond-mat/0201180]
 - [18] P. Butera and M. Comi, Phys. Rev. B **65**, 144431 (2002) [arXiv:hep-lat/0112049]
 - [19] P. Butera and M. Comi, Phys. Rev. B **72**, 014442 (2005) [arXiv:hep-lat/0506001]
 - [20] K. Binder, Z. Phys. B: Condens. Matter **43**, 119 (1981).
 - [21] M. N. Barber Finite-size Scaling in *Phase Transitions and Critical Phenomena*, Vol. 8, eds. C. Domb and J. L. Lebowitz, (Academic Press, 1983)
 - [22] *Finite Size Scaling and Numerical Simulation of Statistical Systems*, ed. V. Privman, (World Scientific, 1990).
 - [23] H. G. Ballesteros, L. A. Fernández, V. Martín-Mayor, A. Muñoz Sudupe, G. Parisi, and J.J. Ruiz-Lorenzo, J. Phys. A **32**, 1 (1999) [arXiv:cond-mat/9805125]

- [24] M. Hasenbusch, K. Pinn, and S. Vinti, Phys. Rev. B **59**, 11471 (1999) [arXiv:hep-lat/9806012]
- [25] M. Hasenbusch, J. Phys. A **32**, 4851 (1999) [arXiv:hep-lat/9902026]
- [26] H. W. J. Blöte, L. N. Shchur, and A. L. Talapov, Int. J. Mod. Phys. C **10**, 1137 (1999) [arXiv:cond-mat/9912005]
- [27] Y. Deng and H. W. J. Blöte, Phys. Rev. E **68**, 036125 (2003).
- [28] M. Hasenbusch, F. Parisen Toldin, A. Pelissetto, and E. Vicari, J. Stat. Mech.: Theory Exp. **2007**, P02016 [arXiv:cond-mat/0611707]
- [29] F. Benitez, J.-P. Blaizot, H. Chaté, B. Delamotte, R. Méndez-Galain, and N. Wschebor, Phys. Rev. E **80** 030103(R) (2009) [arXiv:0901.0128]
- [30] M. Astorino, F. Canfora and G. Giribet, Phys. Lett. B **671**, 291 (2009) [arXiv:0809.1412]
- [31] M. Deserno, Phys. Rev. E **56**, 5204 (1997).
- [32] J. R. Heringa and H. W. J. Blöte, Phys. Rev. E **57**, 4976 (1998).
- [33] Y. Deng and H. W. J. Blöte, Phys. Rev. E **70**, 046111 (2004).
- [34] M. Hasenbusch, Int. J. Mod. Phys. C **12**, 991 (2001).
- [35] H. W. J. Blöte, E. Luijten, and J. R. Heringa, J. Phys. A **28**, 6289 (1995) [arXiv:cond-mat/9509016]
- [36] M. Hasenbusch, Physica A **197**, 423 (1993).
- [37] M. Campostrini, M. Hasenbusch, A. Pelissetto, and E. Vicari, Phys. Rev. B **74**, 144506 (2006) [arXiv:cond-mat/0605083]
- [38] R. C. Brower and P. Tamayo, Phys. Rev. Lett. **62**, 1087 (1989).
- [39] J. A. Plascak, A. M. Ferrenberg, and D. P. Landau, Phys. Rev. E **65**, 066702 (2002) [arXiv:cond-mat/0205264]
- [40] See, e.g., S. Wansleben, J. B. Zabolitzky, and C. Kalle, J. Stat. Phys. **37**, 271 (1984); G. Bhanot, D. Duke, and R. Salvador, Phys. Rev. B **33** 7841 (1986).
- [41] U. Wolff, Phys. Rev. Lett. **62**, 361 (1989).
- [42] M. Hasenbusch, K. Pinn and S. Vinti, Phys. Rev. B **59**, 11471 (1999) [arXiv:hep-lat/9806012]
- [43] M. Saito and M. Matsumoto, “SIMD-oriented Fast Mersenne Twister: a 128-bit Pseudorandom Number Generator”, in *Monte Carlo and Quasi-Monte Carlo Methods 2006*, edited by A. Keller, S. Heinrich, H. Niederreiter, (Springer, 2008); M. Saito, Masters thesis, Math. Dept., Graduate School of science, Hiroshima University, 2007. The source code of the program is provided at “<http://www.math.sci.hiroshima-u.ac.jp/~m-mat/MT/SFMT/index.html>”
- [44] F. Panneton, P. L’Ecuyer, and M. Matsumoto, ACM Transactions on Mathematical Software **32**, 1 (2006). The source code of the program is provided at “<http://www.iro.umontreal.ca/~panneton/WELLRNG.html>”
- [45] K. E. Newman and E. K. Riedel, Phys. Rev. B **30**, 6615 (1984).
- [46] M. Campostrini, A. Pelissetto, P. Rossi and E. Vicari, Phys. Rev. E **57**, 184 (1998) [arXiv:cond-mat/9705086]
- [47] L. A. Fernandez, V. Martin-Mayor, S. Perez-Gaviro, A. Tarancon, and A. P. Young, Phys. Rev. B **80**, 024422 (2009) [arXiv:0905.0322]